High-Pressure MOF Phases

Deutsche Ausgabe: DOI: 10.1002/ange.201506250
Internationale Ausgabe: DOI: 10.1002/anie.201506250

Locating Gases in Porous Materials: Cryogenic Loading of Fuel-Related Gases Into a Sc-based Metal–Organic Framework under Extreme Pressures

*Jorge Sotelo, Christopher H. Woodall, Dave R. Allan, Eugene Gregoryanz, Ross T. Howie, Konstantin V. Kamenev, Michael R. Probert, Paul A. Wright, and Stephen A. Moggach**

Abstract: *An alternative approach to loading metal organic frameworks with gas molecules at high (kbar) pressures is reported. The technique, which uses liquefied gases as pressure transmitting media within a diamond anvil cell along with a single-crystal of a porous metal–organic framework, is demonstrated to have considerable advantages over other gas-loading methods when investigating host–guest interactions. Specifically, loading the metal–organic framework Sc_2BDC_3 with liquefied CO_2 at 2 kbar reveals the presence of three adsorption sites, one previously unreported, and resolves previous inconsistencies between structural data and adsorption isotherms. A further study with supercritical CH_4 at 3–25 kbar demonstrates hyperfilling of the Sc_2BDC_3 and two high-pressure displacive and reversible phase transitions are induced as the filled MOF adapts to reduce the volume of the system.*

Understanding how guest molecules in metal–organic framework (MOFs) interact with each other and the framework they occupy upon adsorption is vital for the development and commercial application of MOFs, for example in carbon capture and gas sequestration technologies.[1] Spectroscopic techniques, such as IR[2] and solid state NMR spectroscopy[3] are often used for probing these interactions. Crystallographic studies, both X-ray and neutron, utilizing various environmental cells have proven invaluable in determining the nature of host–guest interactions within MOFs and their guest-driven structural flexibility.[4] This is particularly important in the many cases where the uptake behavior, which can include conformational changes in the framework itself, can be perturbed by the type and amount of guest adsorbed.[5] One of the main reasons why so little data is available is that the experimental location of gas molecules in MOFs is challenging. The gas molecules are often disordered and exhibit thermal motion which is difficult to model crystallographically even when cooled close to the freezing temperature of the gas adsorbed. In-situ cells have been developed for collecting crystallographic data whilst exposing a MOF to a gaseous environment at tens, or even hundreds of bars of pressure in an effort to saturate the pores with gas molecules, though even here, the gas molecules are often difficult to observe experimentally. For these reasons, despite the intensive research in carbon capture technologies, relatively few crystallographic studies have been reported where CO_2 molecules have been unambiguously located within MOFs.[6]

The use of condensed gases as pressure transmitting media (PTM) in diamond anvil cells is commonplace in the fields of condensed matter physics and high-pressure mineralogy due to their excellent hydrostatic properties at very high pressures (> 10 GPa) relative to common liquid PTMs.[7] He, Ar and Ne are typically used because they are chemically inert, whilst other gases have been studied for their diverse structural behavior. High-temperature and pressure phases of CO_2 and CH_4 are of interest for understanding planetary interiors, for example,[8] while the formation and decomposition of methane hydrates, which are only stable at pressure, has been studied in great detail.[9] Both CO_2 and CH_4 are of obvious industrial and environmental interest.

Here, we present a high-pressure study of the MOF Sc_2BDC_3 (BDC = benzene-1,4-dicarboxylate) using both CO_2 and CH_4 as PTM. Recent work has demonstrated the active role that PTMs play in high-pressure studies of porous materials, where the ability of the PTM to penetrate the framework can be used to "hyperfill"[10] the pores. For example, in a previous study of Sc_2BDC_3 using methanol as a PTM, the pores were hyperfilled with methanol molecules at 16 kbar, achieving a density 2.5 times larger than possible under ambient-pressure conditions.[11] Furthermore, a previous high-pressure study on the zeolitic imidazolate framework, ZIF-8 ($Zn(MeIm)_2$, MeIm = 2-methylimidazole),

[*] J. Sotelo, Dr. S. A. Moggach
EaStChem School of Chemistry and Centre for Science at Extreme Conditions, University of Edinburgh, David Brewster road, Joseph Black Building, Edinburgh EH9 3FJ (UK)
E-mail: smoggach@staffmail.ed.ac.uk
Dr. C. H. Woodall, K. V. Kamenev
School of Engineering and Centre for Science at Extreme Conditions, University of Edinburgh, Peter Gurthrie Tait Road, Erskine Williamson Building, Edinburgh EH9 3FD (UK)
E. Gregoryanz, Dr. R. T. Howie
School of Physics and Centre for Science at Extreme Conditions, University of Edinburgh, Peter Gurthrie Tait Road, Erskine Williamson Building, Edinburgh EH9 3FD (UK)
Dr. M. R. Probert
School of Chemistry, Newcastle University
Newcastle upon Tyne, NE1 7RU (UK)
Dr. D. R. Allan
Diamond Light Source, Harwell Campus, Didcot, OX11 ODE (UK)
Prof. P. A. Wright
EaStCHEM School of Chemistry, Purdie Building, University of St. Andrews, St. Andrews KY16 9ST (UK)

Supporting information for this article is available on the WWW under http://dx.doi.org/10.1002/anie.201506250.

revealed a previously unobserved framework conformation, which has since been used to explain a step in its adsorption isotherm observed for a number of gases, and the increased loading capacity on increasing gas pressure.[12]

In the case of Sc_2BDC_3, gas cell structural work and isotherms by Miller et al. using both CO_2 and CH_4 revealed interesting features worthy of further investigation.[13] Adsorption of CO_2 into Sc_2BDC_3 at 1 bar and 235 K causes a phase transition, which results in a change in space group symmetry from *Fddd* to *C*2/*c*. The transition is characterized by a subtle rotation of one of the two symmetry independent BDC linkers upon exposure to CO_2. This results in three symmetry independent linkers (Group 1, 2a and 2b) and gives rise to two crystallographically independent channels with one absorption site in each channel (Site 1 and Site 2, Figure 1 a). Site 1 lies across two Group 2a linkers with host–guest C–H···O distances of ca. 2.9 Å and Site 2 is disordered over two positions and also has close C–H···O contacts that range from 2.78 to 2.98 Å. At 235 K and 1 atm. Site 1 and Site 2 are fully and half-occupied, respectively, giving a calculated CO_2 adsorption capacity of ca. 3 mmol g^{-1}, which differs significantly from the experimentally measured maximum uptake of 6.5 mmol g^{-1} from adsorption isotherm data (Table 1).

In our current study, CO_2 was compressed to a pressure of 2 kbar within a modified Merrill–Basset DAC, using a multi-state gas compressor containing a single crystal of Sc_2BDC_3 (Supporting Information Figure SI-I). Single-crystal X-ray analysis revealed that upon sealing the DAC, CO_2 entered the MOF, immediately inducing the expected *Fddd* to *C*2/*c* phase transition. At 2 kbar, CO_2 positions appeared similar to those previously observed by Miller et al., with both Site 1 and Site 2 occupied (Figure 1 A). At 2 kbar, Site 1 was fully occupied, and Site 2 was observed to have an occupancy refining to

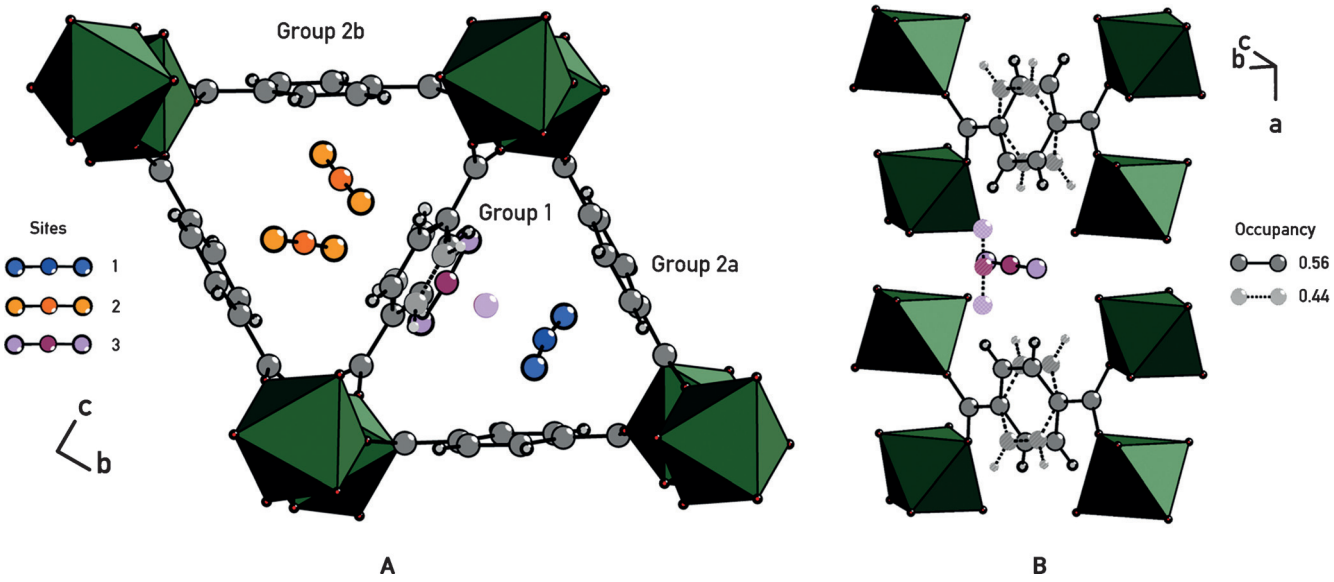

Figure 1. Two different views of the CO_2 included structure of Sc_2BDC_3. A) Positions of the three different adsorption sites (Site 1 in blue, Site 2 in yellow and Site 3 in lilac) as well as the disorder in the framework of Group 1. B) Positional disorder of Site 3 and the Group 1 BDC linker with solid features representing an occupancy of 0.56 and dashed 0.44.

Table 1: Main crystallographic information for the different phases of Sc_2BDC_3 as synthesised, with CO_2 and CH_4 at different pressures.

	Sc_2BDC_3	$Sc_2BDC_3{\cdot}CO_2$ (2 kbar)	$Sc_2BDC_3{\cdot}CH_4$ (3 kbar)	$Sc_2BDC_3{\cdot}CH_4$ (13 kbar)	$Sc_2BDC_3{\cdot}CH_4$ (25 kbar)
Unit cell parameters [Å]	$a=8.7458(3)$ $b=20.7439(6)$ $c=34.349(9)$ $\alpha=90$ $\beta=90$ $\gamma=90$ $V=6231.7(50)$ Å^3	$a=8.693(4)$ $b=34.192(16)$ $c=11.055(5)$ $\alpha=90$ $\beta=111.292(5)$ $\gamma=90$ $V=3062(2)$ Å^3	$a=8.8524(12)$ $b=20.7005(19)$ $c=34.1938(32)$ $\alpha=90$ $\beta=90$ $\gamma=90$ $V=6266(1)$ Å^3	$a=8.8824(7)$ $b=61.2475(33)$ $c=33.6891(20)$ $\alpha=90$ $\beta=90$ $\gamma=90$ $V=18\,328(2)$ Å^3	$a=8.905(2)$ $b=32.501(7)$ $c=10.675(2)$ $\alpha=90$ $\beta=112.05(1)$ $\gamma=90$ $V=2864(1)$ Å^3
Space group	*Fddd*	*C*2/*c*	*Fddd*	*Fdd*2	$P2_1/c$
Wavelength [Å]	0.71 (Mo Kα)	0.56 (Ag)	0.71 (Mo Kα)	0.69 (Zr)	0.69 (Zr)
Completeness	100%	69%	61%	71%	58%
Resolution [Å]	0.84	0.84	0.84	0.84	1.17
R1	0.035	0.107	0.049	0.065	0.145
% SAV[a]	35.7	–	37.4	34.8	29.3
Guest uptake	–	6.2 mmol g^{-1}	7.8 mmol g^{-1}	10.2 mmol g^{-1}	–

[a] SAV = Solvent accessible volume as calculated using Mercury.

0.83(3).[13] The partial occupancy of Site 2 had in previous studies been justified as a form of static disorder, where the two symmetry-related positons of Site 2 could not be occupied simultaneously due to short (< 2.2 Å) intermolecular O–O distances. In the high-pressure structure we report here, the distance between the two symmetry-equivalent sites increased to 2.46 Å, which allows for an increased occupancy for CO_2 at Site 2.

Additionally, a previously undiscovered CO_2 site (Site 3) was observed in the same channel as Site 1 (Figure 1 B). Site 3 was modelled in two orientations, disordered over a two-fold rotation axis. Both positions lie very close to each other (< 0.2 Å apart), discarding the possibility of both being occupied simultaneously. This was confirmed by the refinement of occupancies in the two orientations—0.58(4) when the CO_2 molecule is aligned perpendicular to the channels, and 0.42(4) when parallel to it. Both Site 3 positions lie between sets of Group 1 BDC linkers. The close C–H···O contacts between the phenyl rings and the CO_2 induces a disorder of the Group 1 BDC linkers, which also appear in two orientations (Figure 1 B, Figure SI-III). Refinement of the occupancy of the two orientations of the linker closely matches the obtained values for Site 3 CO_2 molecules (i.e. 0.56(4) and 0.44(4))—indicating the disorder is induced by the presence of the new CO_2 site.

By modelling the new Site 3 and the re-ordering of Site 2, the calculated uptake of CO_2 in Sc_2BDC_3 equates to 6.2 mmol g^{-1}. This value is much closer to the maximum capacity of 6.5 mmol g^{-1} reported by Miller et al., and much better than their previous estimate from their structural work (of 3.4 mmol g^{-1}). This approach also provides direct structural evidence of the expected packing re-arrangement of guest molecules required to reach maximum CO_2 capacity. Application of further pressure beyond 6 kbar resulted in a significant loss of diffraction, most likely due to the freezing of CO_2. Nevertheless, the structural data already obtained exemplified the use of liquefied, near supercritical gases, as an excellent method for "hyper-filling" MOFs, to the extent of allowing the location of all the adsorption sites, including ones not previously visible with X-ray diffraction.

Before, on uptake of CH_4, no phase transition was observed, with the framework retaining the orthorhombic *Fddd* symmetry.[13] At 9 bar and 230 K, a low affinity for CH_4 was observed, with two crystallographically distinct adsorption sites, showing very low fractional occupancy for the C-atom (refined values of 0.15 and 0.25 were obtained for Sites 1 and 2 respectively). This implied that there was potential available capacity in the channels for further adsorption, and motivated us to perform a high-pressure experiment on Sc_2BDC_3 with CH_4 as the PTM.

CH_4 was loaded using a similar principle to CO_2 but using a different method: cryogenically cooling CH_4 to liquefy into the sample chamber of a standard Merrill–Bassett DAC before sealing at 3 kbar (Figure SI-II). The initial loading showed the immediate inclusion of CH_4 molecules inside the framework, and two adsorption sites were found in similar positions to those previously reported but now fully occupied.[13] Site 1 was close to the Group 1 linker (C–H···H–C shortest contact of 2.62 Å), and Site 2 and its symmetry equivalent positions appeared next to Group 2 linkers (C–H···H–C shortest contact of 2.44 Å). Refinement of CH_4 molecules including the hydrogen positions was possible, a rarity in gas adsorption structural studies, and even rarer for high-pressure phases of CH_4 at much higher pressures, where the molecules tend to show several rotational degrees of freedom.[14] The data collected at 3 kbar provided an excellent model for the estimation of the adsorbed CH_4 from the refined occupancies (0.91(2) for Site 1 and 0.68(2) for Site 2) corresponded to 7.8 mmol g^{-1}, beyond the uptake capacity of 6.8 mmol g^{-1} previously reported for Sc_2BDC_3. The increased uptake shown here, beyond what was measured previously provides evidence of hyper-filling the framework at elevated pressures.

It was possible to continue the compression study to 25 kbar before freezing of the CH_4 occurred, resulting in a loss of hydrostaticity and deteriation of diffraction quality. Up until 10 kbar the framework remained unaltered, with CH_4 occupancy of both sites increasing until all sites were fully occupied, yielding a maximum capacity of 10.7 mmol g^{-1}. A small increase in the unit cell volume of < 1 % was observed at 3 kbar, which is a frequent observation in other high-pressure inclusion studies on other MOFs including Sc_2BDC_3.[11,15] As seen with the inclusion of methanol, the expansion seemed to rely mostly on an increase along the *a*-axis, which corresponds to the channel directions (Figure SI-IV). The continued increase of the *a*-axis with increasing pressure is in line with further CH_4 being forced inside the framework, but overall the unit cell volume started to decrease above 6 kbar.

At 10 kbar, an increase in the libration of both Group 1 and 2 BDC linkers was observed, suggesting both linkers were adopting more than one orientation. On increasing pressure to 12 kbar, the appearance of weak reflections indicate the onset of a phase change, which is clear at 13 kbar and results in a tripling of the *b*-axis and reduction in symmetry to *Fdd2* (Figure SI-V). On increasing pressure further to 25 kbar, another phase transition occurs to a previously unobserved form of Sc_2BDC_3 (with the same topology), which has monoclinic symmetry and crystallizes in the space group $P2_1/c$.

Both phase transitions change the pore structure of Sc_2BDC_3. At 13 kbar, the transition from *Fddd* to *Fdd2* results in an increase from one to three different Sc environments. The tripling of the *b*-axis and lowering in symmetry is driven by the rotation of some of the ScO_6 octahedra, with one rotating clockwise, the other anti-clockwise and the last remaining largely unaltered (Figure 2). On increasing pressure further to 25 kbar, the transition from *Fdd*2 to $P2_1/c$ causes a further rotation of the two symmetry independent ScO_6 octahedra. In the final phase, all octahedra are twisted, allowing Sc_2BDC_3 to adopt a higher density form. Analysis of the subgroup-group relations[16] between the three phases shows that the transition from *Fdd*2 and $P2_1/c$ symmetry is forbidden and must go via an unobserved intermediate phase.

These structural changes are coupled to a marginal reduction in the percentage pore volume of Sc_2BDC_3—reducing from 34.9 % to 34.8 % from 3 to 13 kbar respectively, followed by a more significant decrease to 29.2 % in the final

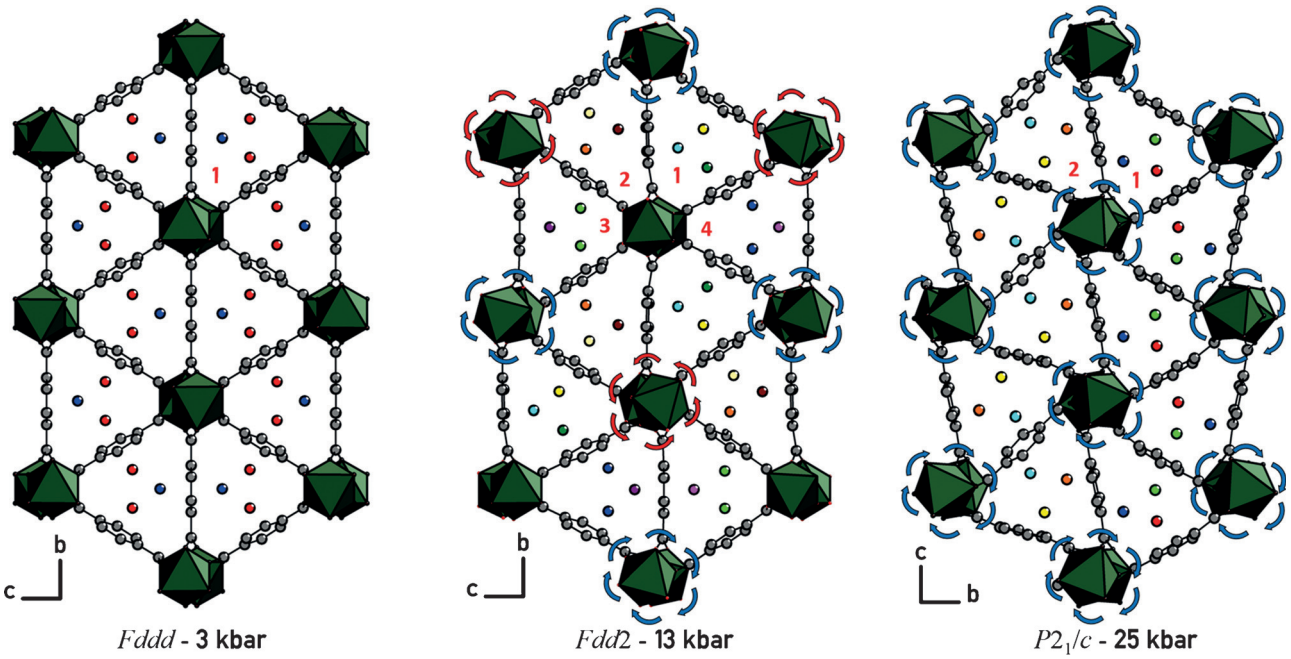

Figure 2. Structural transitions upon high-pressure compression of Sc_2BDC_3 in CH_4. Red and blue arrows represent the rotation of the ScO_6 octahedra for each phase, with red representing anti-clockwise motion and blue clockwise. CH_4 adsorption sites are coloured by symmetry equivalence, with 2, 10, and 6 independent sites in the *Fddd* (left), *Fdd*2 (middle) and $P2_1/c$ (right), respectively. Red numbers represent the different channel types present in each phase change.

phase at 25 kbar. On increasing pressure to 13 kbar, the refined occupancies of the CH_4 molecules decreased, indicating that the amount of CH_4 in the pores started to reduce on undergoing the first phase transition. The driving force for the formation of the high-pressure phases above 10 kbar would therefore appear to be to form denser crystalline phases of Sc_2BDC_3, with CH_4 trapped in the pores. Atomic positions for the CH_4 sites were unambiguously determined for all three phases. In all phases, two different sites per channel were maintained, with a similar arrangement to those observed in the original *Fddd* structure. From fully occupied sites in the *Fddd* structure at 10 kbar, half of the sites in the *Fdd*2 structure at 13 kbar refine to an occupancy of ca. 0.9, revealing a modest reduction in the number of CH_4 molecules upon increasing pressure (Figure SI-V). Unfortunately, extracting definitive conclusions from the pore content analysis in the $P2_1/c$ phase was not possible, since data quality was seriously compromised at such high-pressures, partly due to CH_4 having frozen around the crystal. For this reason, the above mentioned evidence of a reduction in pore volume is the only indication of reduced pore content in the final $P2_1/c$ phase. On decreasing pressure, and recovering the crystal from the pressure cell, the crystal reverts to the original *Fddd* structure.

Overall, these results highlight the potential of using gases as PTM in high-pressure single-crystal diffraction experiments to explore the maximum gas uptake of porous MOFs at room temperature. Not only is it possible to determine adsorption sites within the pores, but the technique also reveals sites unoccupied at lower pressures, where low-uptake or large thermal motion may have made determining guest positions within the pores using diffraction techniques extremely challenging, or impossible. These cryogenic loading DAC studies can be of direct relevance to possible applications of MOFs at high pressures, such as UPLC or the storage of mechanical energy.[17] Finally, this is a new experimental approach to monitoring gas uptake with associated changes in the framework, which are expected to be widely applicable to other MOFs and help obtain improved atomistic models of the gas molecules inside the pores.

Experimental Section

CCDC 1409524–1409530 contain the supplementary crystallographic data for this paper. These data can be obtained free of charge from The Cambridge Crystallographic Data Centre.

Acknowledgements

We thank the EPSRC for funding (EP/K033646) and the STFC for awarding beamtime at the Diamond Light Source.

Keywords: gas separation · high-pressure phases · metal–organic frameworks · structural science · X-ray crystallography

How to cite: *Angew. Chem. Int. Ed.* **2015**, *54*, 13332–13336
Angew. Chem. **2015**, *127*, 13530–13534

[1] a) K. Sumida, D. L. Rogow, J. A. Mason, T. M. McDonald, E. D. Bloch, Z. R. Herm, T. H. Bae, J. R. Long, *Chem. Rev.* **2012**, *112*, 724–781; b) J. R. Li, J. Sculley, H. C. Zhou, *Chem. Rev.* **2012**, *112*, 869–932.

[2] A. Greenaway, B. Gonzalez-Santiago, P. M. Donaldson, M. D. Frogley, G. Cinque, J. Sotelo, S. Moggach, E. Shiko, S. Brandani,

R. F. Howe, P. A. Wright, *Angew. Chem. Int. Ed.* **2014**, *53*, 13483 – 13487; *Angew. Chem.* **2014**, *126*, 13701 – 13705.
[3] H. C. Hoffmann, M. Debowski, P. Muller, S. Paasch, I. Senkovska, S. Kaskel, E. Brunner, *Materials* **2012**, *5*, 2537 – 2572.
[4] E. J. Carrington, I. J. Vitorica-Yrezabal, L. Brammer, *Acta Crystallogr. Sect. B* **2014**, *70*, 404 – 422.
[5] a) C. Serre, C. Mellot-Draznieks, S. Surble, N. Audebrand, Y. Filinchuk, G. Ferey, *Science* **2007**, *315*, 1828 – 1831; b) T. Jacobs, G. O. Lloyd, J.-A. Gertenbach, K. K. Müller-Nedebock, C. Esterhuysen, L. J. Barbour, *Angew. Chem. Int. Ed.* **2012**, *51*, 4913 – 4916; *Angew. Chem.* **2012**, *124*, 4997 – 5000.
[6] a) S. Takamizawa, E.-i. Nakata, T. Saito, K. Kojima, *CrystEngComm* **2003**, *5*, 411 – 413; b) Y.-Q. Tian, Y.-M. Zhao, H.-J. Xu, C.-Y. Chi, *Inorg. Chem.* **2007**, *46*, 1612 – 1616; c) J. P. Zhang, X. M. Chen, *J. Am. Chem. Soc.* **2009**, *131*, 5516 – 5521; d) S. Takamizawa, Y. Takasaki, R. Miyake, *Chem. Commun.* **2009**, 6625 – 6627; e) R. Vaidhyanathan, S. S. Iremonger, G. K. H. Shimizu, P. G. Boyd, S. Alavi, T. K. Woo, *Science* **2010**, *330*, 650 – 653; f) M. Wriedt, J. P. Sculley, A. A. Yakovenko, Y. Ma, G. J. Halder, P. B. Balbuena, H.-C. Zhou, *Angew. Chem. Int. Ed.* **2012**, *51*, 9804 – 9808; *Angew. Chem.* **2012**, *124*, 9942 – 9946; g) S. Xiang, Y. He, Z. Zhang, H. Wu, W. Zhou, R. Krishna, B. Chen, *Nat. Commun.* **2012**, *3*, 954; h) S. Couck, E. Gobechiya, C. E. Kirschhock, P. Serra-Crespo, J. Juan-Alcaniz, A. Martinez Joaristi, E. Stavitski, J. Gascon, F. Kapteijn, G. V. Baron, J. F. Denayer, *ChemSusChem* **2012**, *5*, 740 – 750; i) W. Kosaka, K. Yamagishi, A. Hori, H. Sato, R. Matsuda, S. Kitagawa, M. Takata, H. Miyasaka, *J. Am. Chem. Soc.* **2013**, *135*, 18469 – 18480; j) P. Zhao, G. I. Lampronti, G. O. Lloyd, M. T. Wharmby, S. Facq, A. K. Cheetham, S. A. Redfern, *Chem. Mater.* **2014**, *26*, 1767 – 1769; k) W. L. Queen, M. R. Hudson, E. D. Bloch, J. A. Mason, M. I. Gonzalez, J. S. Lee, D. Gygi, J. D. Howe, K. Lee, T. A. Darwish, M. James, V. K. Peterson, S. J. Teat, B. Smit, J. B. Neaton, J. R. Long, C. M. Brown, *Chem. Sci.* **2014**, *5*, 4569 – 4581.
[7] a) M. Eremets, *High Pressure Experimental Methods*, Oxford Science Publications, **1996**; b) S. Klotz, J. Chervin, P. Munsch, G. Le Marchand, *J. Phys. D* **2009**, *42*, 075413.
[8] J. Matson in *Scientific American*, Nature Publishing Group, **2011**.
[9] N. Pantha, N. P. Adhikari, S. Scandolo, *High Pressure Res.* **2015**, 1 – 8.
[10] K. W. Chapman, G. J. Halder, P. J. Chupas, *J. Am. Chem. Soc.* **2008**, *130*, 10524 – 10526.
[11] A. J. Graham, A. M. Banu, T. Duren, A. Greenaway, S. C. McKellar, J. P. S. Mowat, K. Ward, P. A. Wright, S. A. Moggach, *J. Am. Chem. Soc.* **2014**, *136*, 8606 – 8613.
[12] a) S. A. Moggach, T. D. Bennett, A. K. Cheetham, *Angew. Chem. Int. Ed.* **2009**, *48*, 7087 – 7089; *Angew. Chem.* **2009**, *121*, 7221 – 7223; b) D. Fairen-Jimenez, S. A. Moggach, M. T. Wharmby, P. A. Wright, S. Parsons, T. Duren, *J. Am. Chem. Soc.* **2011**, *133*, 8900 – 8902; c) D. Fairen-Jimenez, R. Galvelis, A. Torrisi, A. D. Gellan, M. T. Wharmby, P. A. Wright, C. Mellot-Draznieks, T. Duren, *Dalton Trans.* **2012**, *41*, 10752 – 10762; d) C. O. Ania, E. García-Pérez, M. Haro, J. J. Gutiérrez-Sevillano, T. Valdés-Solís, J. B. Parra, S. Calero, *J. Phys. Chem. Lett.* **2012**, *3*, 1159 – 1164.
[13] S. R. Miller, P. A. Wright, T. Devic, C. Serre, G. Ferey, P. L. Llewellyn, R. Denoyel, L. Gaberova, Y. Filinchuk, *Langmuir* **2009**, *25*, 3618 – 3626.
[14] H. E. Maynard-Casely, L. F. Lundegaard, I. Loa, M. I. McMahon, E. Gregoryanz, R. J. Nelmes, J. S. Loveday, *J. Chem. Phys.* **2014**, *141*, 234313.
[15] A. J. Graham, D. R. Allan, A. Muszkiewicz, C. A. Morrison, S. A. Moggach, *Angew. Chem. Int. Ed.* **2011**, *50*, 11138 – 11141; *Angew. Chem.* **2011**, *123*, 11334 – 11337.
[16] M. I. Aroyo, J. M. Perez-Mato, D. Orobengoa, E. Tasci, G. de La Flor, A. Kirov, *Bulg. Chem. Commun.* **2011**, *43*, 183 – 197.
[17] S.-S. Liu, C.-X. Yang, S.-W. Wang, X.-P. Yan, *Analyst* **2012**, *137*, 816 – 818.

Received: July 7, 2015
Published online: September 11, 2015